Differential Regulation of Noxa in Normal Melanocytes and Melanoma Cells by Proteasome Inhibition: Therapeutic Implications

Yolanda Fernández,[1] Monique Verhaegen,[1] Thomas P. Miller,[1] Jenny L. Rush,[2] Philipp Steiner,[4] Anthony W. Opipari, Jr.,[3] Scott W. Lowe,[5] and María S. Soengas[1]

Departments of [1]Dermatology, [2]Chemistry, and [3]Obstetrics and Gynecology, University of Michigan Comprehensive Cancer Center, Ann Arbor, Michigan; [4]Millennium Pharmaceuticals, Inc., Cambridge, Massachusetts; and [5]Cold Spring Harbor Laboratory, Cold Spring Harbor, New York

Abstract

Melanoma is the most aggressive form of skin cancer and advanced stages are invariably resistant to conventional therapeutic agents. Using bortezomib as a prototypic proteasome inhibitor, we have identified a novel and critical role of the proteasome in the maintenance of the malignant phenotype of melanoma cells that could have direct translational implications. Thus, melanoma cells from early, intermediate, and late stages of the disease could not sustain proteasome inhibition and underwent an effective activation of caspase-dependent and -independent death programs. This effect was tumor cell selective, because under similar conditions, normal melanocytes remained viable. Intriguingly, and despite of interfering with a cellular machinery in charge of controlling the half-life of the vast majority of cellular proteins, bortezomib did not promote a generalized disruption of melanoma-associated survival factors (including NF-κB, Bcl-2, Bcl-x_L, XIAP, TRAF-2, or FLIP). Instead, we identified a dramatic induction *in vitro* and *in vivo* of the BH3-only protein Noxa in melanoma cells (but not in normal melanocytes) in response to proteasome inhibition. RNA interference validated a critical role of Noxa for the cytotoxic effect of bortezomib. Notably, the proteasome-dependent regulation of Noxa was found to extend to other tumor types, and it could not be recapitulated by standard chemotherapeutic drugs. In summary, our results revealed Noxa as a new biomarker to gauge the efficacy of bortezomib specifically in tumor cells, and provide a new strategy to overcome tumor chemoresistance. (Cancer Res 2005; 65(14): 6294-304)

Introduction

Melanoma is a prime example of a chemoresistant tumor type (1–4). Complete response rates with dacarbazine (DTIC), the only drug approved by the U.S. Food and Drug Administration (FDA) for the treatment of metastatic melanoma, rarely exceed 5% (5). Moreover, combination cocktails of DTIC with agents aimed to kill tumor cells by alkylation, cross-linking, ribonucleotide depletion, microtubule destabilization, or topoisomerase inhibition, among many others, have failed to significantly improve long-term survival of patients with metastatic disease (6, 7).

The rational design of improved therapeutics has been complicated by the complexity of genetic alterations acquired during melanoma progression (2). Hyperactivation of efflux pumps, detoxification enzymes, and a multifactorial alteration of survival and apoptotic pathways have been proposed to mediate the multidrug-resistant (MDR) phenotype of melanoma cells (3, 4). However, no factor has been consistently identified as a gold-standard marker for melanoma progression or melanoma maintenance.

Agents with pleiotropic effects that are able to interfere simultaneously with the expression (and function) of survival and apoptotic factors may offer an alternative to standard single-target drugs. In this context, the proteasome inhibitor bortezomib (Velcade, previously known as PS-341) is raising great enthusiasm as a new class of anticancer agent that is not subject to classic MDR-dependent inactivation (8, 9). Bortezomib has a wide spectrum of action in hematologic and solid tumors, including lung, breast, prostate, pancreatic, and head and neck carcinomas (9, 10). Based on its efficacy, the FDA has approved the use of bortezomib for the treatment of refractory multiple myeloma (11), and several clinical trials are under way testing its therapeutic value in a variety of cancers (12, 13).

Interestingly, intratumoral injections of bortezomib have been recently reported to reduce the localized growth of human melanoma xenografts in mice, particularly when combined with the DTIC derivative temozolomide (14). Important questions remain as to the mechanistic basis underlying the higher sensitivity of melanoma cells than normal melanocytes to bortezomib. In fact, the proteasome controls the half-life of the vast majority of cellular proteins (15), and it has been rather puzzling that proteasome inhibitors such as bortezomib can be clinically effective while displaying an acceptable safety profile. Thus, although bortezomib is generally considered a potent inducer of cell death, the mechanism(s) underlying its tumor cell selectivity is poorly understood (even in tumor types where bortezomib is being tested in clinical settings; ref. 9). Up-regulation of proapoptotic factors such as Bax (16) and down-regulation of the antiapoptotic proteins Bcl-2, Bcl-x_L, XIAP, and FLIP, in part through the inactivation of the nuclear factor-κB (NF-κB) pathway, have been proposed as frequent facilitators of cell death in bortezomib-treated tumor cells (17–22). However, whether these changes in expression are cause or consequence of the death process and whether they are general mediators of the cytotoxic effect of bortezomib is unclear (9).

Note: Supplementary data for this article are available at Cancer Research Online (http://cancerres.aacrjournals.org/).

P. Steiner is currently at the ImClone Systems, Inc., New York.

Requests for reprints: María S. Soengas, University of Michigan Comprehensive Cancer Center (4217 CCGC), 1500 East Medical Center Drive, Ann Arbor, MI 48109. Phone: 734-936-5643; Fax: 734-647-9654; E-mail: soengas@umich.edu.

Here we report on a comprehensive analysis of the effect of bortezomib on the apoptotic machinery of normal melanocytes and a panel of 23 melanoma lines. Standard chemotherapeutic agents with different cellular targets (Adriamycin and cisplatin) were analyzed in parallel to reveal events that may be uniquely activated by bortezomib in tumor cells. We identify a novel mechanism of action of bortezomib in melanoma and other tumor cells that depends on the induction of the proapoptotic protein Noxa. This work is an important step in understanding how melanoma chemoresistance can be overcome by blocking protective signals dependent on the proteasome that maintain the apoptotic machinery of melanoma cells in a dormant state.

Materials and Methods

Cells. Normal melanocytes were isolated from neonatal foreskins as reported elsewhere (23). Radial growth phase cell lines WM-35, WM-155C, and WM-1789 (herein coded as R1, R2, and R3) and vertical growth phase line WM-278, WM-793, WM-902B, and WM-1366 (V1, V2, V3, and V4) were kindly provided by Dr. Meenhard Herlyn at the Wistar Institute (Philadelphia, PA). For consistency, the metastatic melanoma series SK-Mel-5, SK-Mel-19, SK-Mel-28, SK-Mel-29, SK-Mel-94, SK-Mel-103, SK-Mel-147, SK-Mel-173; G-361, Malme-3M, and UACC-62 and UACC-167 were referred to with codes used in a previous publication: codes 2, 3, 4, 5, 7, 9, 10, 11, 14, 15, 17, and 18, respectively (see Supplementary Table S1 and ref. 24 for additional information). Lines MM-426, MM-603, MM-608, and MM-622 included in the Supplementary Information were a generous gift of Nicholas Hayward (Human Genetics Laboratory, Queensland Institute of Medical Research).

Reagents. Bortezomib (Velcade, formerly PS-341) was obtained from Millennium Pharmaceuticals (Cambridge, MA). For analyses of cell death and cell cycle in tissue culture systems, bortezomib was reconstituted in DMSO at a concentration of 0.1 mmol/L; for studies *in vivo*, it was prepared in a 0.85% (w/v) sterile saline solution. Adriamycin (doxorubicin) and cisplatin were obtained from Sigma Chemical (St Louis, MO).

Cell viability assays. The percentage of death cells at the indicated times and drug concentrations was estimated by standard trypan blue exclusion or 3-(4,5-dimethyl thiazol-2-yl)-2,5-diphenyl tetrazolium bromide assays as described elsewhere (25). For simplicity, control samples, which were incubated only with solvent (0.05-0.1% DMSO), are indicated as nontreated. Analysis of chromatin condensation and cellular ultrastructure by electron microscopy are indicated in the Supplementary Information.

Cell cycle analyses. Normal melanocytes or melanoma cells (5×10^5) were treated with bortezomib (50 nmol/L) or vehicle control. Cell cycle analyses were conducted after a 2-hour incubation of cells in labeling solution (50 μg/mL of propidium iodide (PI; Sigma Chemical), in PBS containing 0.2% Triton and 10 μg/mL RNase A. PI fluorescence was measured using a FACSCalibur. Cell cycle distribution was determined with a Cell Quest software (Becton Dickinson, San Jose, CA).

Protein immunoblots. To determine changes in protein levels, 2×10^6 cells were treated with Adriamycin (0.5 μg/mL), bortezomib (50 nmol/L), or cisplatin (30 μg/mL) and harvested at the indicated time points. Total cell lysates were subjected to electrophoresis in 12%, 15%, or 4% to 15% gradient SDS gels under reducing conditions, and subsequently transferred to Immobilon-P membranes (Millipore, Bedford, MA). Protein bands were detected by enhanced chemiluminescence system (see Supplementary Information for a list of the antibodies used in this study). Cytosolic and membrane-rich fractions were prepared by digitonin extraction essentially as previously described (26). Cytosolic fractions (100 μg) and 25 μg of mitochondrial fractions were used to visualize Cyt *c*, Smac, HtrA2, and AIF release by Western blotting. Control antibodies were COX IV for the mitochondrial fraction and β-actin for the cytosolic fraction.

Fluorometric caspase activity assays. Protein (20 μg) of cytosolic fraction from the digitonin fractionation were incubated with 200 μL of Activation Buffer [50 mmol/L Pipes (pH 6.85), 0.1 mmol/L EDTA, 10% glycerol, 1 mmol/L DTT] in the presence of 20 μmol/L of one of the following 7-amino-4-trifluoromethyl coumarin (AFC) derivatives: Ac-LEHD (preferentially cleaved by Casp-9, Casp-5, and related cystein proteases), Ac-IETD (as a preferred substrate of Casp-8, Casp-6), or Ac-DEVD (preferentially cleaved by Casp-3, Casp-7, and related caspases). Proteolytic release of AFC was monitored as indicated by the provider (Biomol Research, Plymouth Meeting, PA) at a λ_{exc} = 400 nm and λ_{em} = 505 nm using a CytoFluor Multiwell Plate Reader Series 4000 (Applied Biosystems, Framingham, MA). Signal was expressed as arbitrary fluorescent units (AFU)/min. Experiments were done in triplicate.

Stable RNA interference. To down-regulate the expression of Noxa by RNA interference (RNAi), oligonucleotides allowing for the generation of 19-bp short hairpin RNAs (shRNA) were designed following indications by the OligoRetriever Database (http://katahdin.cshl.org:9331/RNAi_web/scripts/main2.pl). BLAST search was done to ensure at least 4-nucleotide (nt) differences with annotated human genes. The corresponding oligonucleotides were annealed and cloned under the control of the H1 promoter into a self-inactivating lentiviral vector (27). The vector was also designed to carry the green fluorescent protein reporter gene under control of the human ubiquitin-C promoter to monitor infection efficiency. Lentiviral infections were done essentially as described elsewhere (27) and the potency and specificity of each construct was determined by protein immunoblotting (see text). The constructs generated were as follows: Noxa (1), nt 1177 to 1195 and Noxa (2), nt 295 to 313. Scrambled oligonucleotides were also designed to generate control shRNA. Cloning strategies and primer sequences are available from the authors on request.

Quantitative real-time PCR. Total RNA from cultured cells was obtained by using the RNeasy Mini Kit (Qiagen, Inc., Chatsworth, CA). Total RNA (0.5 μg) was reverse-transcribed using the Superscript III reverse transcription kit (Invitrogen, Carlsbad, CA). Relative mRNA levels of *Noxa* and the housekeeping gene *β-actin* were determined by reverse transcription-PCR (RT-PCR) using a LightCycler DNA Master SYBR Green I kit (Roche Diagnostics GmbH, Mannheim, Germany) and an automated PCR station (BioMek 2000, Beckman-Coulter, Miami, FL). Typical amplification reactions (15 μL) contained 2.5 mmol/L $MgCl_2$, 0.6 μmol/L of a primer mix, 1.5 μL of SYBR Green Mix, and one tenth of the reverse transcription reaction. A 7700 Sequence Detector (Applied Biosystems) was programmed for an initial step of 5 minutes at 95°C followed by 35 cycles of 30 seconds at 95°C, 30 seconds at 60°C, and 30 seconds at 72°C. The oligonucleotides used as specific primers for *Noxa* were 5′-ATGAATGCACCTTCACATTCCTCT (sense) and 5′-TCCAGCAGAGCTGGAAGTCGAGTGT (antisense). Fluorescence was automatically monitored during every PCR cycle and during the post-PCR temperature ramp. For each sample, RNA content was normalized to *β-actin*. Fluorescence values were expressed with respect to the basal expression of nontreated normal melanocytes. The specificity of PCR amplification of each primer pair was confirmed by analyzing PCR products by agarose gel electrophoresis and by melting curve analysis.

Melanoma growth *in vivo* (mouse xenografts). Female athymic nude mice (Taconic Farms, Germantown, NY) were kept in pathogen-free conditions and used at 8 to 12 weeks of age. Animal care was provided in accordance with the procedures outlined in the Guide for the Care and Use of Laboratory Animals of the University of Michigan. To analyze localized growth of melanoma cells *in vivo*, 0.5×10^6 melanoma cells were injected s.c. in both rear flanks (n = 10 tumors per experimental condition). Treatment was initiated 48 hours after tumor implantation. Bortezomib was given systemically by i.p. injection (1.0-1.3 mg/kg) in a rotating 2-day schedule. Similar results were obtained for treatments done via i.v. administration (data not shown). Animals were weighed every 2 days to ensure maintenance of total weight within 80% of control populations. Tumor volume was estimated as $V = L \times W^2 / 2$, where L and W stand for tumor length and width, respectively. Tumors were collected at day 17 postinjection and snap frozen; 0.4-μm sections were prepared for histologic analyses to guide with manual microdissection (to restrict tissue specimens to areas with >70% tumor cellularity) for subsequent protein isolation.

Statistics. Statistical analysis of tumor growth *in vivo* was done using the Statistical Package of the Social Sciences (SPSS) version 11.5 for Windows. Nonparametric Mann-Whitney U test was used for two-group comparisons. Two-tailed $P < 0.05$ was considered statistically significant.

Results

Higher efficacy and selectivity of bortezomib than standard chemotherapeutic drugs Adriamycin and cisplatin. To begin to address the efficacy of bortezomib, changes in cell viability were analyzed in three independent populations of normal human skin melanocytes and 16 well-characterized cell lines isolated from early (radial growth phase), intermediate (vertical growth phase), and late stages of the disease (metastasis; refs. 24–28). Adriamycin, a DNA-damaging agent known for its poor efficacy against melanoma (29), was also compared in parallel to identify mechanistic aspects of bortezomib that are not shared by standard chemotherapeutic agents. Drug concentrations were selected to maintain death rates of melanocytes below 30%.

Adriamycin was able to kill the "early-stage" radial growth phase cells, but most vertical growth phase and metastatic lines were resistant (see relative death rates in Fig. 1*A* and dose-response curves for representative examples of metastatic lines in Fig. 1*B, left*). In contrast, all lines died after bortezomib treatment (Fig. 1*A-B*). These include aggressive lines such as, for example, lines 9 and 10, expressing low levels of Apaf-1 and high levels of antiapoptotic factors such as Bcl-2, Bcl-x_L, Mcl-1, or Survivin (see Supplementary Table 1). Similarly, melanoma-associated mutations in *p53, Ras, B-Raf*, or the *INK4a/ARF* locus did not compromise the response to bortezomib (Fig. 1*A*; Supplementary Table S1). The tumor cell–selective effect of bortezomib was illustrated by a death rate below 30% of normal melanocytes (even at doses of 100 nmol/L, 10 times the EC_{50} for melanoma cells; Fig. 1*B, middle*). Interestingly, analysis of cell cycle progression by standard flow cytometry assays indicated that melanocytes did in fact respond to bortezomib and stop proliferating at the G_2-M

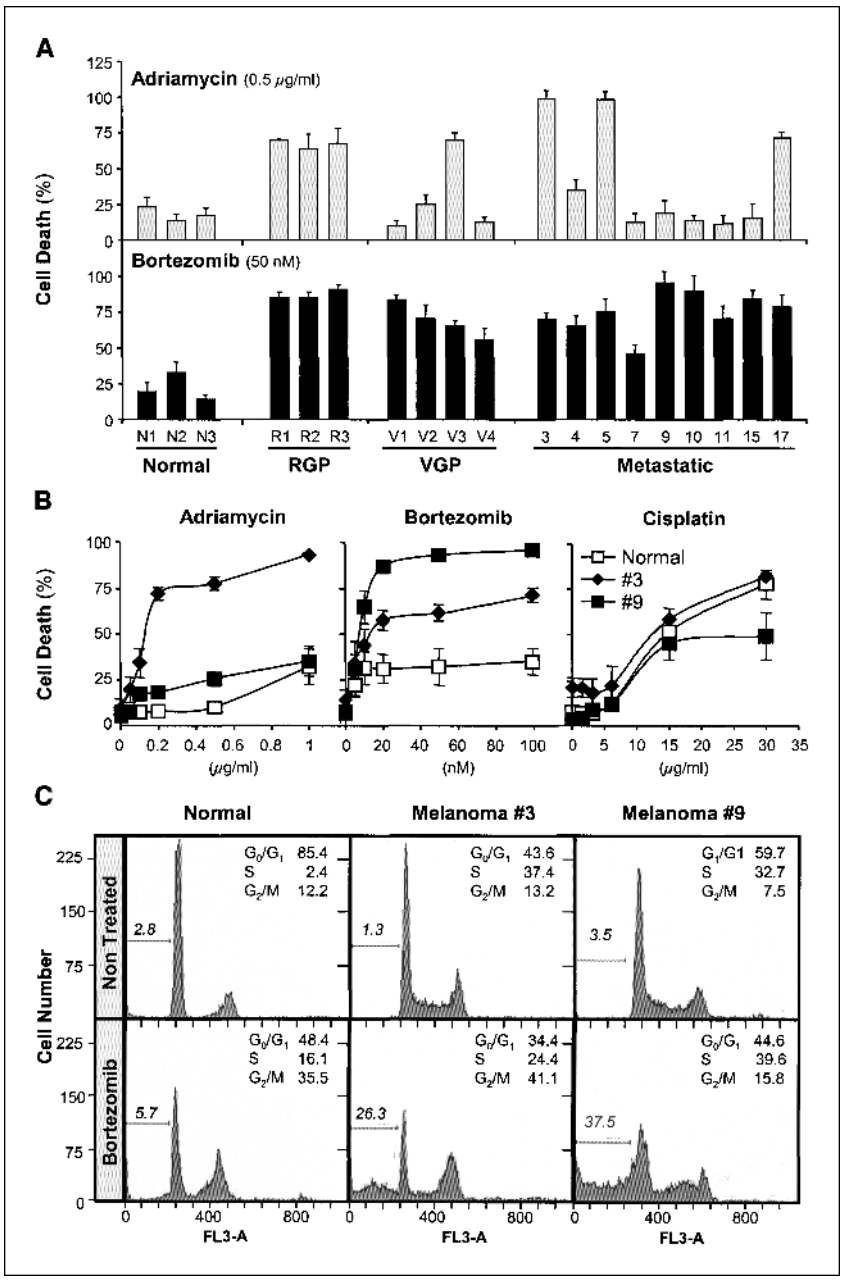

Figure 1. Efficacy and selectivity of bortezomib. *A,* cell death induced by Adriamycin and bortezomib on a panel of melanoma cell lines with different functional status or expression of melanoma-associated genes. See Materials and Methods for the code number used to refer to each cell line and Supplementary Table 1 for the genetic background of the metastatic cells. Cell death was estimated by trypan blue exclusion 36 hours after treatment. *B,* dose-response curves of bortezomib and the chemotherapeutic drugs Adriamycin and cisplatin on normal foreskin melanocytes (*Normal*) and metastatic melanoma cells (cell lines 3 and 9), 36 hours after treatment. *C,* cell cycle distribution determined by flow cytometry of the indicated melanoma cells treated with solvent ("Non Treated") or with 50 nmol/L bortezomib for 24 hours. The amount (%) cells with fragmented DNA (sub-G_0-G_1) is shown in italics. For each experimental condition shown is also the percentage of viable cells at the G_0-G_1, S, and G_2-M phases of the cell cycle.

phases of the cycle (Fig. 1*C, left*). However, whereas normal melanocytes and remained viable, melanoma cells seemed to have fragmented DNA (measured as a sub-G_0 population; Fig. 1*C*).

We next determined the relative efficacy of bortezomib with respect to more effective inducers of melanoma cell death. The melanoma lines used in this study are highly resistant to DTIC (>600 μg/mL); therefore, we focused on cisplatin as an example of a drug frequently used in melanoma clinical trials (30–31). As indicated in Fig. 1*B* (*right*), cisplatin was able to kill both Adriamycin-sensitive and -resistant lines, but in contrast to bortezomib, it was highly toxic for normal melanocytes and hence not selective.

Activation of extrinsic and intrinsic apoptotic pathways by bortezomib. 4′,6-Diamidino-2-phenylindole (DAPI) staining and electron microscopy revealed classic apoptotic hallmarks in bortezomib-treated melanoma cells (such as chromatin condensation, membrane blebbing, and maintenance of the integrity of cellular membranes; see Supplementary Fig. S1). Therefore, we focused on apoptotic pathways to address the mechanism of action of bortezomib and to determine quantitative and/or qualitative differences with Adriamycin and cisplatin.

Caspase processing and activation were assessed in five representative cell lines. Metastatic lines 3 and 5 are sensitive to DNA-damaging agents and process regulatory (Casp-9 and Casp-8) and effector caspases (Casp-3 and Casp-7) after Adriamycin treatment (Fig. 2*A*). The vertical growth phase line V4 and the metastatic lines 9 and 10 are more resistant to Adriamycin, and as previously described (24) have an impaired caspase activity (see Fig. 2*A*). Interestingly, all lines cleaved regulatory and effector caspases in response to bortezomib (Fig. 2*A*). Standard fluorescence-based proteolytic assays indicated that caspases processed in response to bortezomib were in fact functional (Fig. 2*B*). The response to cisplatin, however, was more heterogeneous. Thus, cisplatin-induced cell death did not

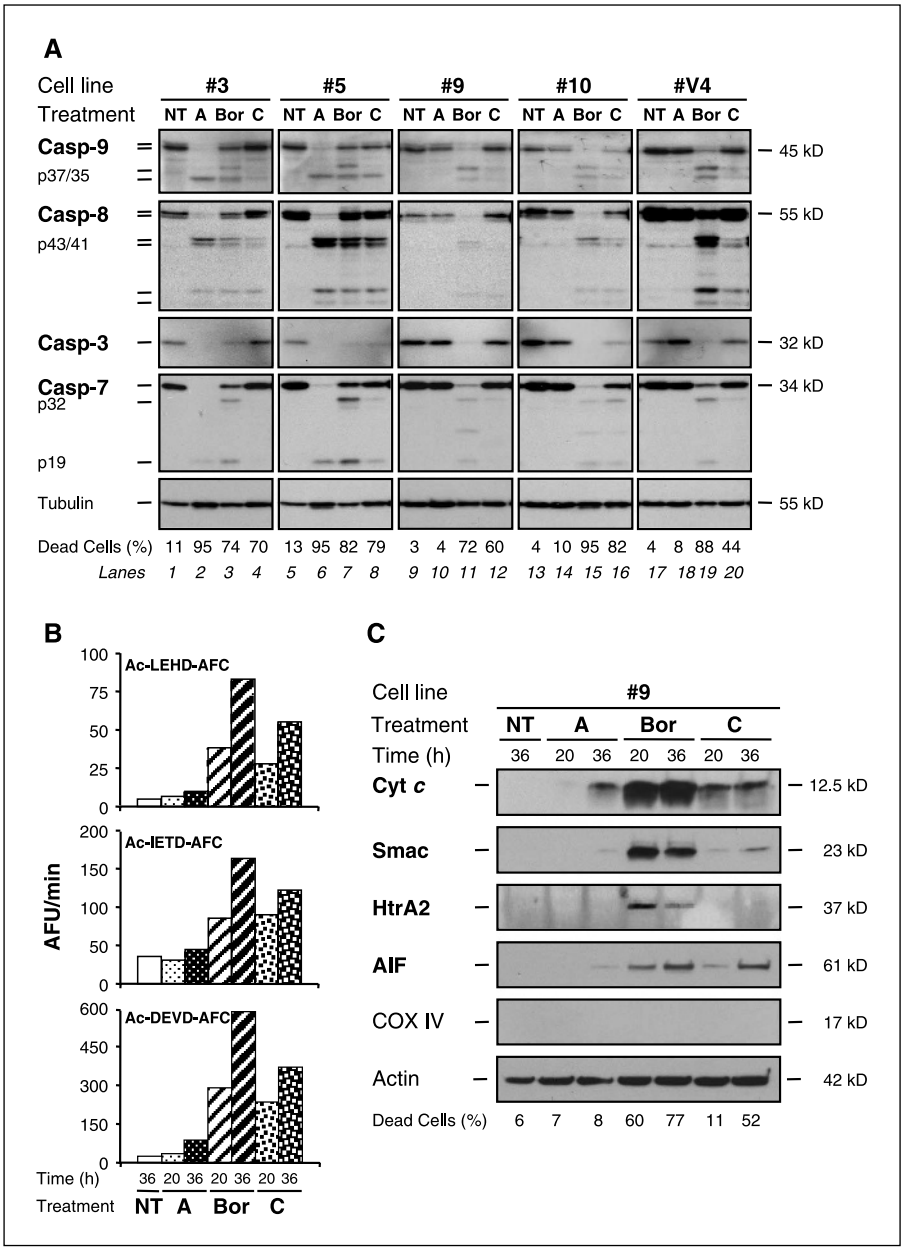

Figure 2. Apoptotic features of bortezomib-induced cell death. *A,* comparative ability of Adriamycin (*A*, 0.5 μg/mL), bortezomib (*Bor*, 50 nmol/L), and cisplatin (*C*, 30 μg/mL) to process apoptotic caspases. Total cell lysates were separated in a 15% PAGE-gel and probed for the indicated antibodies. NT stands for control cell populations incubated just in the presence of solvent (0.05% DMSO). *B,* analysis of caspase activation at 20 and 36 hours after treatment using caspase fluorogenic substrates (Ac-LEHD-AFC, Ac-IETD-AFC, and Ac-DEVD-AFC, respectively) in digitonin-fractionated cytosolic extracts. *C,* higher potency of bortezomib than Adriamycin or cisplatin to promote release of the indicated death inducers from the mitochondria. The immunoblots correspond to cytosolic extracts prepared as in (*B*). COX IV, an inner mitochondrial membrane protein was used as a control for the absence of contamination of mitochondrial proteins in the cytosolic extracts.

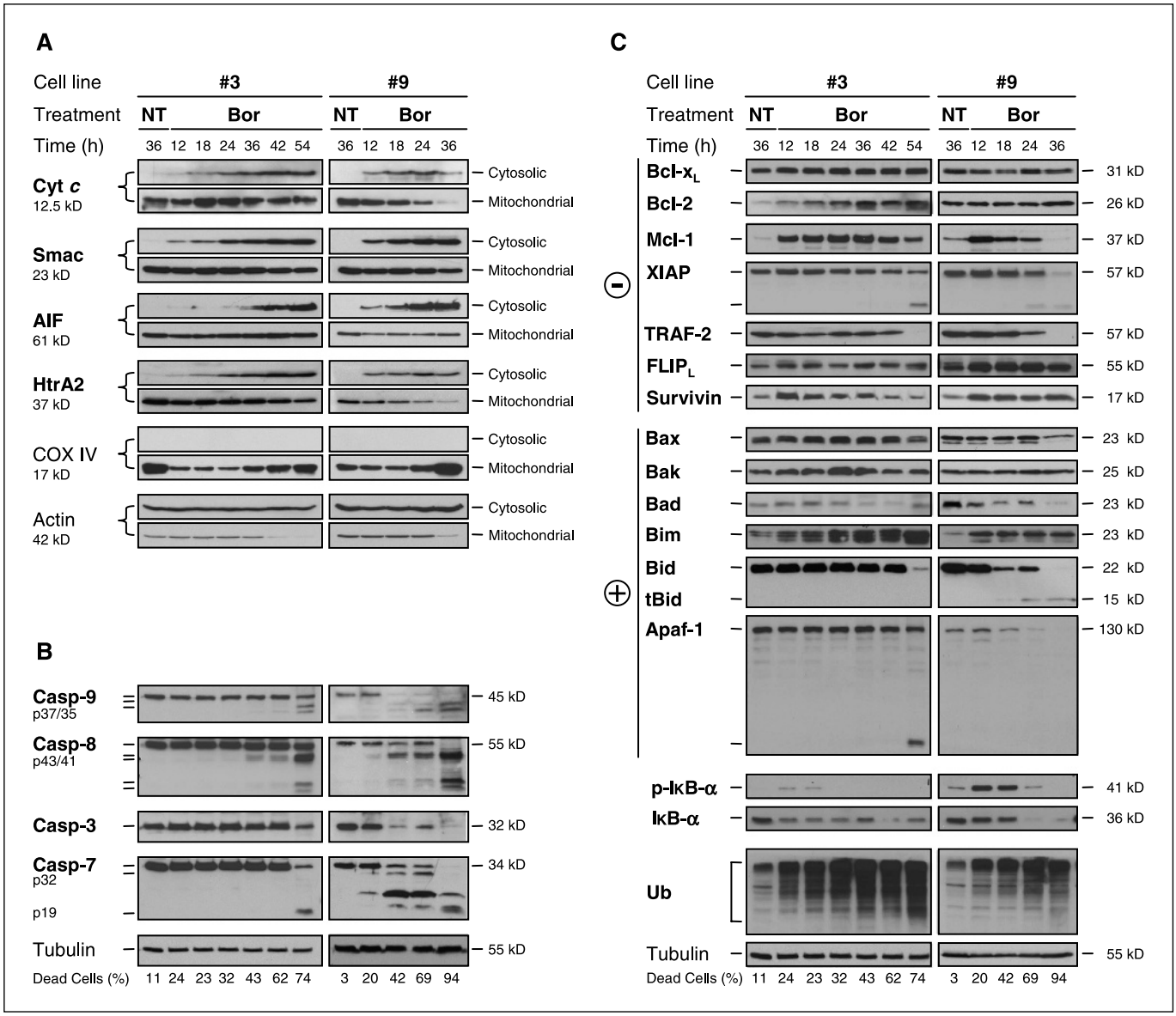

Figure 3. Modulation of apoptotic effectors and regulators by bortezomib. *A,* cell population-based kinetic analysis of the release of Cyt *c*, Smac, HtrA2, and AIF from the mitochondria into the cytosol in control (nontreated, *NT*) and bortezomib-treated melanoma cells (*Bor*, 50 nmol/L) determined by digitonin-based subcellular fractionation. Shown are representative PAGE-SDS gels. *B,* total extracts from melanoma cells treated as in (*A*) were prepared and subjected to immunoblotting for the analysis of regulatory and effector caspases. The extent of cell death at each experimental time point was determined by trypan blue and indicated as a reference. *C,* time course analysis of changes in the expression of antiapoptotic (−) and proapoptotic (+) factors after bortezomib treatment. Phosphorylated and total IκB-α and ubiquitinated proteins (*Ub*) are also shown as a reference.

necessarily correlate with caspase processing. Note for example an 80% killing with a barely detectable processing of Casp-9, Casp-8, and Casp-3 in cisplatin-treated lines 3 or 10 (Fig. 2*A, lanes 4* and *16*), respectively).

In summary, Adriamycin, cisplatin, and bortezomib differed in their ability to activate apoptotic caspases. Moreover, cellular fractionation studies showed a higher efficacy of bortezomib than Adriamycin or cisplatin to promote the release Cyt *c* and Smac from the mitochondria to the cytosol (Fig. 2*C*). In addition, bortezomib promoted the release of the mitochondrial proteins HtrA2 and AIF (Fig. 2*C*). HtrA2 and AIF in turn, could further favor the activation of caspase-independent death pathways (32), which may be important contributors to the cytotoxic effect of bortezomib because the pan-caspase inhibitor zVAD-fmk reduces but cannot completely abrogate cell killing by this proteasome inhibitor (see Supplementary Fig. S2).

Changes in the levels of apoptotic factors frequently associated with the nuclear factor-κB pathway do not precede Cyt *c* release nor caspase activation. Time courses were done to monitor the release of death inducers from the mitochondria and identify early events involved in the activation of apoptotic pathways. To this end, enriched cytosolic and membrane-enriched fractions were prepared from control untreated and bortezomib-treated cells and changes in protein expression were determined as a function of time (see Fig. 3 for representative examples of metastatic melanoma lines 3 and 9). Using this strategy, the release of Cyt *c*, Smac, and HtrA2 was detectable 12 to 18 hours after treatment (Fig. 3*A*).

A series of candidate proteins were then analyzed to identify those whose expression was affected before 12 to 18 hours upon bortezomib treatment. According to other systems, expected results were to find a down-regulation of antiapoptotic factors such as Bcl-x_L, Bcl-2, FLIP, XIAP, cIAP1, cIAP2, or TRAF-2 before Cyt *c* release. However, as shown in Fig. 3*C*, that was not the case in melanoma cells. In fact, XIAP, cIAP1, cIAP2, or TRAF-2 were processed *after* caspases became activated (Fig. 3*C*; results not shown). Moreover, Cyt *c* release proceeded despite a massive up-regulation of the antiapoptotic Mcl-1, which in other systems has to be down-regulated to allow for the induction of apoptotic cell death (33).

Inhibition of the NF-κB has also been shown to favor bortezomib-induced caspase in some, although not all, tumor types (9, 10). Reporter plasmids containing canonical NF-κB binding sites showed no significant inhibition of the intrinsic basal transcriptional activity of NF-κB by bortezomib in the melanoma cells tested in this study (see Supplementary Fig. S3). Consistent with these results, the total amount of IκB, a NF-κB inhibitor, did not significantly change during bortezomib treatment (Fig. 3*C*). Proteasome inhibition however could in fact block the exogenous activation of NF-κB (e.g., by tumor necrosis factor-α, TNF-α; see Supplementary Fig. S3).

With respect to proapoptotic factors, no consistent up-regulation was found for Bax or Bak by bortezomib (Fig. 3*C*). Moreover, cell death was not favored by an increase of Apaf-1 levels; in fact, this protein was cleaved during treatment (Fig. 3*C*). Bim was found to be induced by bortezomib (Fig. 3*C*). However, this protein was also up-regulated by bortezomib in normal melanocytes, which remained viable (see Supplementary Fig. S4).

An alternative mechanism that could account for Cyt *c* is the activation of the death receptor pathway via Casp-8-mediated Bid cleavage (34). However, Bid processing was detected substantially *after* the release of Cyt *c* (Fig. 3*A* and *C*). Therefore, it is also unlikely that Bid is an initial trigger of mitochondrial dysfunction in bortezomib-induced melanoma death.

In summary, bortezomib-mediated release of mitochondrial death inducers is not preceded in melanoma cells by a significant cleavage of Bid nor a NF-κB-dependent down-regulation of Bcl-2, Bcl-x_L, XIAP, FLIP, or TRAF-2, all previously associated with melanoma chemoresistance (3, 24).

Stress-associated signals are not early drivers of the selectivity of bortezomib towards melanoma cells. A regulated release of Cyt *c* can be also be favored by the activation of a series of stress-related signals that can be controlled by the proteasome. These include the unfolded protein response (UPR) at the endoplasmic reticulum and the induction of stress kinases such as p38 and c-*jun* NH_2-terminal kinase (JNK; ref. 10). In melanoma cells, the classic UPR proapoptotic factor CHOP and the chaperone Grp-78 can be induced by bortezomib (Fig. 4*A*). However, the up-regulation of CHOP was found also in normal melanocytes, and did not correlate with the extent of cell death. The induction of Grp-78 was detectable at late time points after bortezomib treatment (Fig. 4*A*). Similarly, melanoma cells are not dependent on JNK or p38 function to respond to bortezomib by inducing apoptosis. Pharmacologic inhibitors of p38 (PD-169316, SB-220025, SB-239063, and SC-68376) and JNK kinases (SP-600125, D-JNK peptide inhibitor 1, or L-JNK peptide inhibitor 1) were unable to protect melanoma cells from bortezomib's killing. Moreover, these inhibitors increased the toxicity of bortezomib on normal melanocytes.

Novel mode of action of bortezomib. Tumor cell–selective activation of Noxa. The proteasome controls the half-life of 80% of cellular proteins. To guide in the identification of key factors induced in response to proteasome inhibition, a comparative analysis of cell cycle and apoptotic inducers was done to identify changes in gene expression showing a maximal difference between normal melanocytes and melanoma cells.[6] From this study, the BH3-only Noxa was identified as the strongest candidate to mediate the tumor-selective effect of bortezomib. Thus, total cell extracts of untreated and bortezomib-treated melanoma cells showed a dramatic up-regulation of Noxa protein (>50-fold). This induction was observed as early as 3 to 6 hours after bortezomib treatment (see Fig. 4*A* for representative example of lines 3 and 9) and before the mitochondrial membrane potential of melanoma cells was affected (data not shown). More importantly, the up-regulation of Noxa was restricted to tumor cells, for it remained undetectable in normal melanocytes. Melanocytes however did accumulate ubiquitinated proteins, as well as other classic proteasome targets such as Hsp70, Mcl-1, and p53, at similar rates than melanoma cells (Fig. 4*A*; Supplementary Fig. S4).

To determine whether induction of Noxa by bortezomib is a general event in melanoma cells, a total of 16 metastatic melanoma lines independently isolated and with different genetic backgrounds (24, 35) were analyzed. As shown in Supplementary Fig. S5, 15 of these 16 lines accumulated Noxa at early time points after treatment. Intriguingly, despite Noxa being reported as a p53 target (36, 37), the accumulation of Noxa by bortezomib is likely p53-independent because it was also observed in melanoma lines such as line 4 (SK-Mel-28), expressing the inactive R273H p53 mutant. Defects in the p53 regulator $p14^{ARF}$ (e.g., lines 10, 15, or 17) did not compromise Noxa up-regulation (see Supplementary Fig. S5). Of note, Noxa has been described as able to promote the release of Cyt *c* without inducing large-range swelling of isolated mitochondria (38), and p53-independent induction of Noxa has been previously reported in melanoma cells (39).

Drug-selective activation of Noxa by bortezomib. Parallel treatments of melanoma lines 3 and 9 with Adriamycin, cisplatin, and bortezomib showed a drastic difference in the effect on these different drugs on Noxa expression. Compare for example the 2- to 3-fold induction of Noxa by Adriamycin or cisplatin (visualized after long exposures of protein immunoblots) with >75-fold induction by bortezomib (Fig. 4*B*). Supporting a p53-independent regulation of Noxa in melanoma cells, the levels of Noxa and p53 showed no directly correlation. As shown in Fig. 4*B*, the accumulation of p53 was higher in lines treated with Adriamycin and cisplatin than with bortezomib.

Transcriptional up-regulation of Noxa by bortezomib. The accumulation of Noxa by bortezomib could be a simple response of blockage of protein degradation or involve activation of gene expression. To this end, quantitative RT-PCR (see Materials and Methods) was done in normal melanocytes and melanoma lines 3 and 9, at time t = 0, 1, 3, 6, 12, and 24 hours after bortezomib treatment. *β-actin* was used as control housekeeping gene whose expression is not modulated by bortezomib (see Fig. 3*A*). As shown in Fig. 5*A*, the intrinsic levels of *Noxa* mRNA in melanoma cells (t = 0 hour) were found to be 2- to 6-fold higher than in

[6] Y.F. and M.S.S., unpublished results.

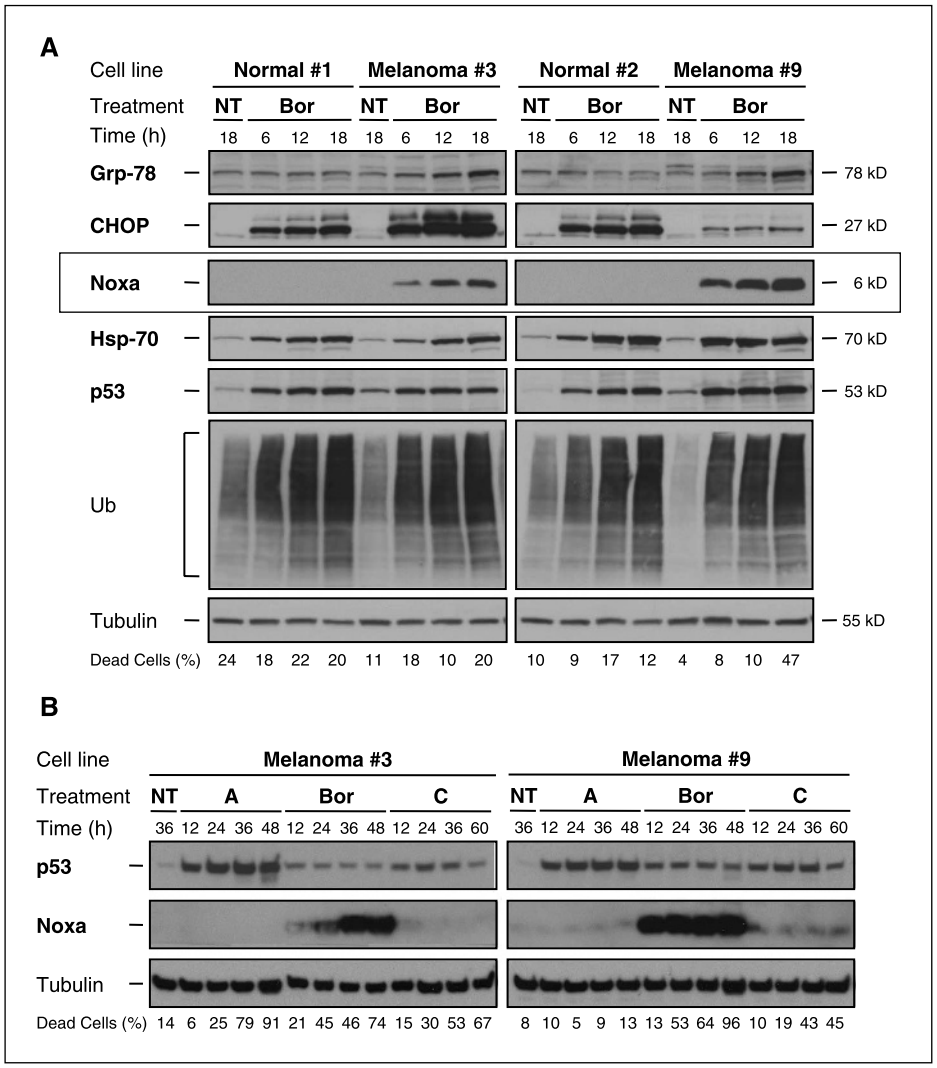

Figure 4. Tumor- and drug-selective up-regulation of Noxa by bortezomib. *A,* identification of factors selectively up-regulated in response to bortezomib (50 nmol/L) in two independent populations of normal foreskin melanocytes (*Normal 1* and *2*) and melanoma lines 3 and 9. Total cell lysates were separated into 4% to 20% PAGE-SDS gels to determine the relative levels of the indicated proteins at early time points after treatment. Note the tumor-selective induction of Noxa, while Hsp-70, p53, and ubiquitinated proteins (*Ub*) are induced in both normal and tumor cells. *B,* differential effect of Adriamycin (*A*, 0.5 μg/mL), cisplatin (*C*, 30 μg/mL), and bortezomib (*Bor*, 50 nmol/L) on p53 and Noxa determined by protein immunobloting. Tubulin is shown as a loading control.

normal melanocytes, with the highest expression in the most sensitive line 9. Bortezomib treatment induced a further accumulation of Noxa mRNA more effectively in the tumor cells than normal melanocytes. For example, whereas at 12 hours posttreatment a 4-fold increase of mRNA levels was detected in normal melanocytes, melanoma lines 3 and 9 expressed 42- and 57-fold higher Noxa mRNA than the untreated normal controls (Fig. 5*A*). Therefore, the tumor-selective up-regulation of Noxa may rely on higher endogenous mRNA levels in melanoma cells than normal melanocytes, further augmented during treatment by new mRNA and protein synthesis.

RNA interference validated a critical role of Noxa for the cytotoxic effect of bortezomib. Given the effect of bortezomib on Noxa mRNA levels, short hairpin interfering RNA constructs (shRNA) were stably expressed into melanoma cells by means of lentiviral vectors to block the induction of Noxa and to establish its requirement for bortezomib's toxicity. Two independent shRNA mapping in the 3′ untranslated region and coding sequence of Noxa, herein referred as Noxa (1) and Noxa (2), were found to significantly knockdown Noxa protein up-regulation by bortezomib (98% and 72%, respectively). The levels of other Bcl-2 family members such as Bcl-2 or Bcl-x_L were not affected by Noxa shRNA expression (Fig. 5*B*). Both constructs compromised the efficacy of bortezomib, delaying its kinetics (data not shown) and decreasing the sensitivity to this proteasome inhibitor (Fig. 5*C*). For example, note a 50% reduction in the amount of cell death of Noxa-defective line 9 at 25 or 50 nmol/L bortezomib (Fig. 5*C*). Similar inhibitory effects were found in lines 3 and 10 (data not shown). Therefore, these results confirmed a critical role of Noxa as an early inducer of the cytotoxic effect of bortezomib in melanoma cells.

Bortezomib-mediated up-regulation of Noxa *in vivo*. Altogether, our results support Noxa expression as a surrogate to address early events driven by bortezomib in melanoma cells. To confirm this hypothesis, the activation of Noxa was analyzed *in vivo*, by monitoring changes in gene expression in melanoma cells grown as mouse xenografts. Of the panel of cell lines shown in Fig. 1, lines 9 and 10 were chosen on the basis of displaying the most aggressive growth after s.c. implantation in immunosuppressed mice (data not shown). Bortezomib has been recently shown to block melanoma growth in mice when injected peritumorally (14). To better recapitulate administration routes used in the clinic, mice were treated systemically with bortezomib or placebo control as indicated in Materials and Methods. Although bortezomib will have to be potentiated with additional chemotherapeutic agents, it noticeably reduced tumor growth (see Fig. 6*A, a-b*; Supplementary Fig. S6). Histologic evaluation of

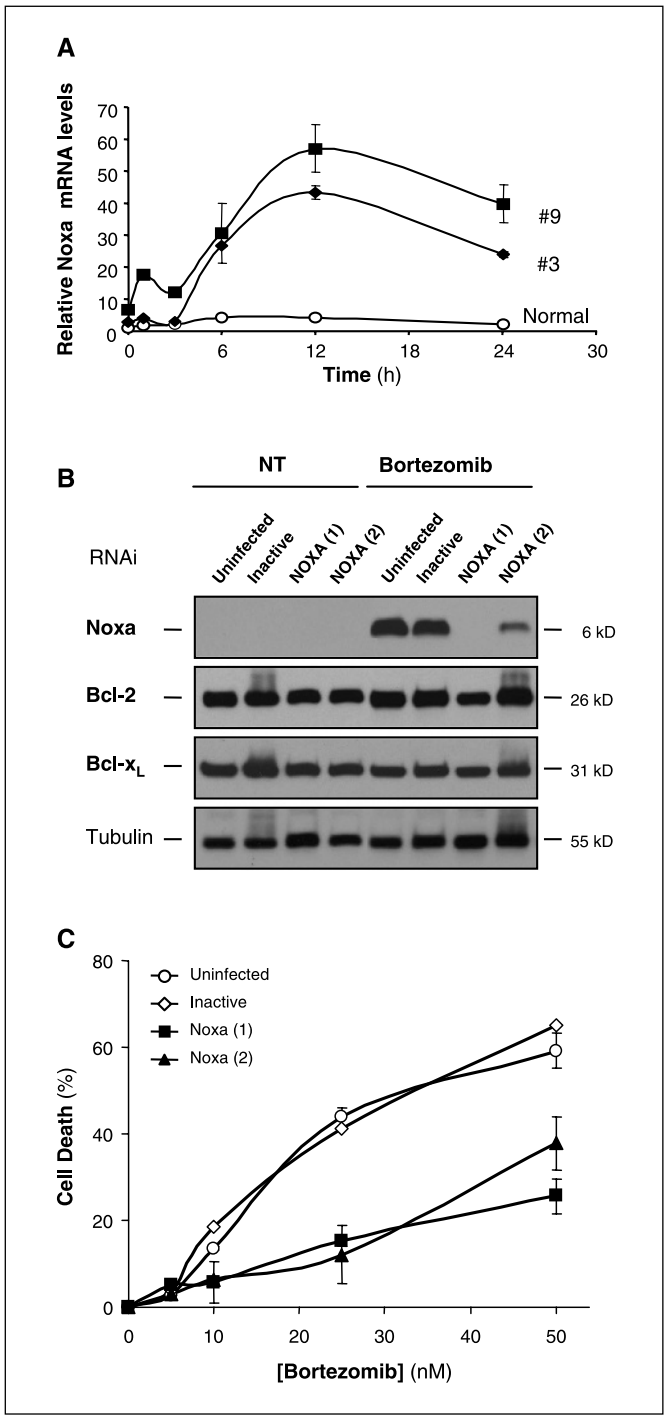

Figure 5. Up-regulation of *Noxa* mRNA expression by bortezomib and its inactivation by RNAi. *A,* relative amount of *Noxa* mRNA in normal melanocytes and melanoma cells 3 and 9. Expression levels were determined by quantitative RT-PCR, normalized to an internal control (*β-actin*), and represented with respect to the basal levels in untreated melanocytes. *Point,* average of triplicates; *bars,* ±SD. *B,* validation of the effect of Noxa on the cytotoxic effect of bortezomib. Analysis of gene expression in melanoma line 9 uninfected or 2 days after infection with lentiviral vectors expressing inactive shRNA or shRNA for Noxa nt 1177 to 1195 (1) or nt 295 to 313 (2). The indicated cell populations were treated with 50 nmol/L bortezomib and total cell extracts were collected 24 hours after treatment and the expression of Noxa was determined by immunoblotting. Bcl-2 and Bcl-x_L are shown as controls for unspecific effects of the lentiviral vectors. *C,* dose-response curves determined 24 hours after treatment showing a significant reduction in the sensitivity to bortezomib by the RNAi against Noxa. The amount of cell death (%) was quantified by trypan blue exclusion.

untreated and bortezomib-treated xenografts (Fig 6*A, c-f*) showed a noticeable reduction of mitotic figures and changes in the tumor architecture (with increased fibrotic areas and tumor cell collapse). More importantly, protein extracts prepared from the tumor xenografts revealed a clear induction of Noxa by bortezomib *in vivo* (Fig. 6*B*). Therefore, our results provide the proof of concept for the use of Noxa as biomarker to address proteasome inhibition in tumor cells.

The activation of Noxa by bortezomib is not exclusive to melanoma cells. To determine whether the induction of bortezomib could be generalized to other tumor types, Jurkat, MDA-MB-231, and H460 were chosen as examples of tumor lines of different cellular origin (T-cell leukemia, breast cancer, and non–small cell lung cancer, respectively). As shown in Fig. 7, Noxa was accumulated in all these cell lines, particularly in MDA-MB-231 cells. Further emphasizing a p53-independent regulation of Noxa by bortezomib, Jurkat and MDA-MB-231 are deficient for p53 (see Fig. 7). Therefore, Noxa represents the first tumor-selective proapoptotic inducer found activated by bortezomib but not by conventional chemotherapeutic agents and involved in the response to this proteasome inhibitor in different tumor types, including those expressing p53 mutations.

Discussion

Here we describe a new role of the proteasome in the maintenance of the malignant phenotype of melanoma cells. Using bortezomib as the "first-in-class" proteasome inhibitor in clinical trials (9), we show an unanticipated dependence of human melanoma cells on the proteasome to block the expression of BH3-only protein Noxa and to prevent the spontaneous activation of apoptosis. Importantly, this dependence is highly restricted to tumor cells, providing a window for therapeutic intervention. The fact that Noxa could not be up-regulated by Adriamycin or cisplatin emphasizes a mechanism of action of bortezomib that is quantitatively and qualitatively different from standard chemotherapeutic agents, which are notoriously ineffective in melanoma.

Unexpected mechanism underlying the efficacy and selectivity of bortezomib. The proteasome controls the half-life of the vast majority of cellular proteins. Therefore, identifying the main drivers of bortezomib's toxicity within a myriad of inconsequential byproducts of proteasome inhibition has been a major challenge in all tumor types where this drug has been tested (9, 10). Consequently, it is not surprising that gold-standard markers of early events induced by bortezomib in a tumor-selective manner have remained elusive (9).

Perhaps one of the most intriguing results of this study is that bortezomib was able to promote an effective release of Cyt *c* and other mitochondrial death inducers without down-regulating protective signals dependent on Bcl-2, Bcl-x_L, XIAP, TRAF-2, or FLIP, frequently associated with melanoma chemoresistance. Therefore, and in contrast to multiple myeloma, lymphoma, Hodgkin disease, or pancreatic or lung cancer cells (18, 19, 40–42), our data is not consistent with a proteasome/IκB-dependent regulation of the above indicated antiapoptotic factors. In addition, reporter plasmids containing canonical NF-κB binding sites indicated that although bortezomib was able to block exogenous activation for example by TNF-α, its effects on the basal transcriptional activity of NF-κB were not statistically significant. It should be noted that our functional analyses of NF-κB activation (Supplementary Fig. S3) are compatible with those of Amiri et al.

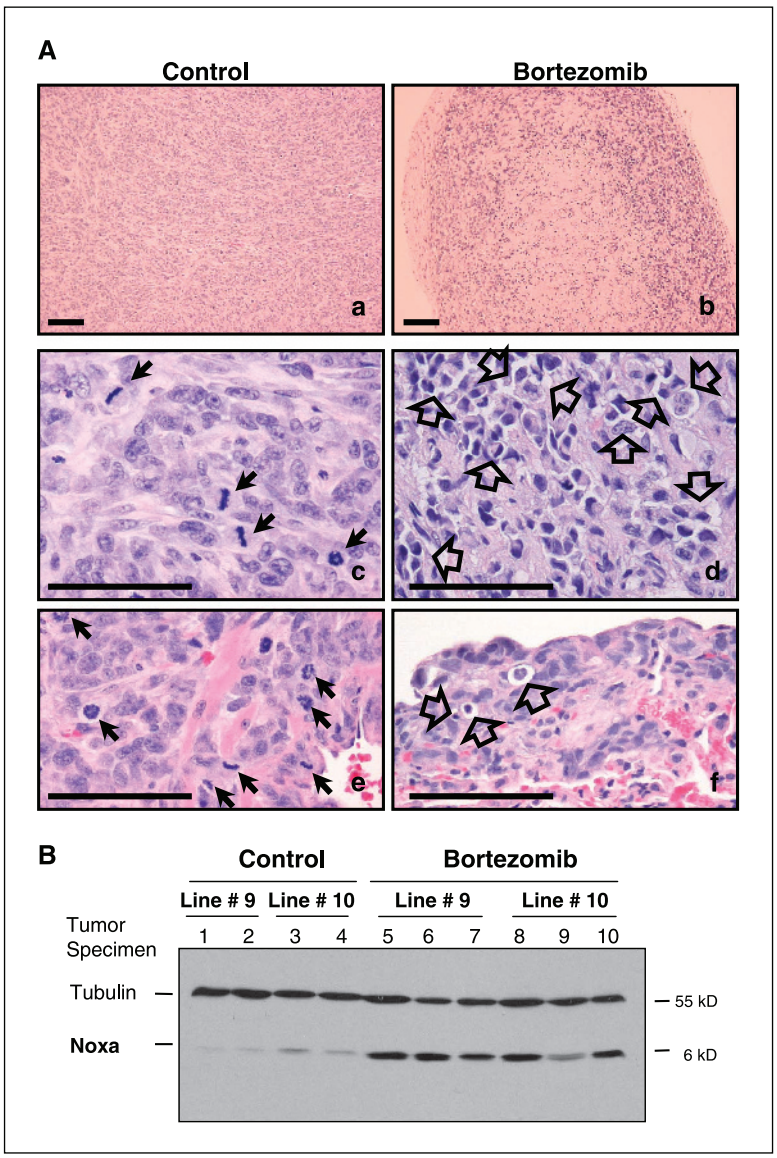

Figure 6. Drug response and induction of Noxa *in vivo*. *A,* histologic analyses of bortezomib treatment in melanoma cells grown as xenografts in immunocompromised mice. H&E staining of paraffin-embedded sections prepared from tumors generated by melanoma line 9 at day 17 after treatment with placebo control (*a*) or bortezomib (*b*). Note the reduced cellularity of the treated specimens (*b*). Photographs were taken at a 10× magnification. See Supplementary Fig. S6 for whole-body imaging of tumor growth of animals inoculated with melanoma lines 9 or 10. *c-f,* visualization of the effect of bortezomib on cell proliferation and viability (40× magnification). Mitotic figures (*black arrows*) clearly evident in control specimens (*c* and *e*) are absent in treated tumors (*d* and *f*), which in contrast showed a large fraction of collapsed cells and picnotic nuclei (*transparent arrows*). *B,* Noxa as a biomarker for Bortezomib action *in vivo*. Total cell lysates (30 μg) isolated from the indicated tumor specimens were separated by PAGE and transferred to Immobilon-P membranes. Noxa and the loading control Tubulin were simultaneously visualized by staining with specific antibodies.

(14). These authors found a limited effect of bortezomib on the intrinsic levels of the NF-κB targets such as CXCL8 or MDR-1, but a compensatory effect upon Temozolomide treatment. Our results however do not support the hypothesis of caspase activation driven by the down-regulation of antiapoptotic factors controlled by NF-κB.

In addition, a comprehensive analysis of the effect of bortezomib the dissipation of the mitochondrial membrane permeability, induction of JNK- and p38-dependent stress pathways did not support these events as initiating or rate-limiting drivers of the selective effect of bortezomib. In marked contrast, Noxa was identified for the fist time as an early gene specifically restricted to tumor cells and whose inactivation by RNAi significantly affected the kinetics and dose-response of bortezomib.

The apoptotic machinery in melanoma cells: kept in a dormant state? Melanoma has been invariably linked to defective apoptotic pathways and multidrug resistance (4). However, the similar sensitivities shown here for bortezomib on a large panel of cell lines independently isolated from early, intermediate, and late stages of the disease, clearly indicate that despite multiple genetic and epigenetic defects accumulated during tumor progression, melanoma cells still retain the core machinery to engage the activation of the apoptotic caspases. An important corollary of this study is that neither high levels of antiapopotic Bcl-2 family members, nor classic melanoma-associated mutations in *N-Ras, B-Raf, p53*, and the *INK4a/ARF* locus, as well as increased levels of Survivin (see Supplementary Table S1) can prevent melanoma cell death if the proteasome is blocked. Similarly, although low Apaf-1 levels can compromise the response of melanoma cells to Adriamycin (24, 43), Paclitaxel (44), and high doses of etoposide (45), this is not the case for bortezomib. Because none of the lines in this study is completely deficient for Apaf-1 (see Table 1 and ref. 24), it is conceivable that the high levels of cytosolic Cyt *c* and Smac released by bortezomib in response to Noxa compensate for reduced Apaf-1 expression and/or high levels of antiapoptotic signals that may prevent caspase activation (e.g., high levels of XIAP or Ml-IAP). The release of AIF and of HtrA2 from the mitochondria could further contribute to caspase-independent death events, particularly if caspases are inactivated (Supplementary Fig. S2). It should be noted that

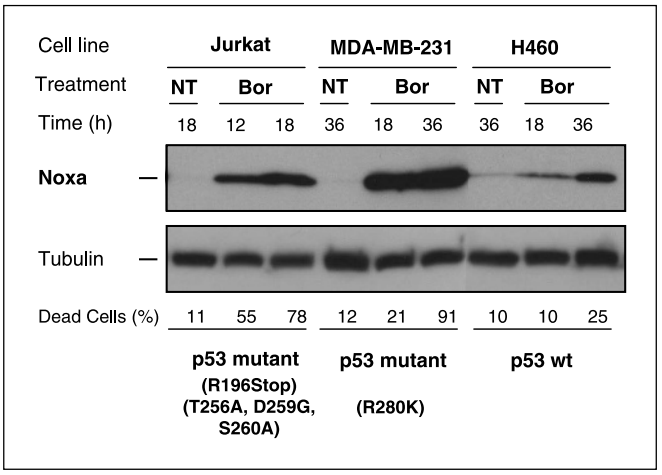

Figure 7. Activation of Noxa by bortezomib in other tumor types. The ability of bortezomib to induce Noxa extends to cell lines isolated from T-cell leukemia (Jurkat), breast cancer (MDA-MD-231), and non–small lung cancer (H460). Cells were treated with solvent (nontreated, *NT*) or 50 nmol/L bortezomib (*Bor*) and processed at the indicated times to detect Noxa by immunoblotting. The percentage of dead cells at each experimental time point was determined by trypan blue and indicated as a reference. Shown is also the status of p53 in the three cell lines as indicated in published references (47).

cisplatin can also bypass low Apaf-1 expression (e.g., in lines 9 or 10). Nevertheless, at the doses required to activate the death machinery, cisplatin is also toxic for normal melanocytes and thus not selective.

At face value, the dramatic up-regulation of Noxa in response to proteasome inhibition, and the subsequent release of proapoptotic factors from the mitochondria underscore a critical role of the proteasome in maintaining apoptotic programs in a latent or suppressed state. In this context, melanoma cells may be more dependent on proteasomal degradation than normal melanocytes because they need to repress their intrinsically high levels of Noxa mRNA. It could be argued that oncogenic transformation drives the activation of a proteasome-controlled transcription factor able to transactivate Noxa and/or stabilize its mRNA. In keeping with this view, and as described for proapoptotic functions of c-Myc or E2F-1 (46), the accumulation of Noxa as a "byproduct" of tumor development may serve as the Achilles' heel for the selective destruction of malignant cells.

Noxa as a biomarker of proteasome inhibition. Given the pleiotropic nature of the proteasome, it would not be expected that Noxa is the *sole* initiator of the cytotoxic effect of bortezomib. Thus, we have shown both by flow cytometry in cultured cells and by histologic analyses in tissue specimens, that bortezomib can effectively interfere with cell cycle progression. Still, and precisely because the large fraction of proteins that could have been affected by this inhibitor, a 50% reduction in cell death observed by RNAi against a single gene (*Noxa*) is highly significant. Moreover, our results could have potential clinical implications. As indicated before, bortezomib is being actively tested in clinical trials against multiple tumor types, but no marker has been consistently identified to address drug efficacy specifically in tumor cells. Here we showed a generalized accumulation of Noxa in 15 of 16 metastatic melanoma lines tested, as well as in cell lines from T-cell leukemia, breast, and non–small cell lung cancer (Jurkat, MDA-MB-321, and H460, respectively). Therefore, based on the dramatic difference in expression between tumor and normal cells (>50-fold induction), we propose Noxa as a novel biomarker to address proteasome inhibition specifically in tumor cells. In addition, we have shown the induction of Noxa in archived frozen specimens from tumor xenografts treated *in vivo*. Therefore, the possibility of analyzing Noxa by immunologic approaches may facilitate a systematic analysis of tumor-specific proteasome inhibition on biopsies collected pretreatment and posttreatment. Furthermore, the fact that Noxa can be up-regulated in p53 mutant lines [e.g., SK-Mel-28 (here referred as melanoma 4), Jurkat, or MDA-MB-231] support the use of this BH3-only protein as a surrogate for proteasome inhibition even in p53-defective tumor types.

In summary, this study has revealed a novel mechanism to activate the latent apoptotic machinery of melanoma cells that cannot be recapitulated by Adriamycin and cisplatin, as examples of two drugs with different modes of action. Moreover, bortezomib has served as powerful experimental tool to address the interplay between the proteasome and proapoptotic and antiapoptotic factors acting upstream, downstream and at the level of the mitochondria. Our results identify Noxa as a new marker to assess the effect of bortezomib *in vitro* and *in vivo* and provide the basis for the rational design of novel therapeutics to overcome tumor chemoresistance by exploiting intrinsic differences in the requirement of the proteasome for the maintenance of the viability of normal and tumor cells.

Acknowledgments

Received 2/28/2005; revised 4/11/2005; accepted 4/20/2005.

Grant support: Dermatology Foundation Career Development Award (M.S. Soengas); grants NIH R01 CA107237 (M.S. Soengas), CA10456 (A.W. Opipari), and CA13106 (S.W. Lowe); Spanish Ministry of Education and Science postdoctoral fellowship (Y. Fernández); and V Foundation for Cancer Research scholarship (M.S. Soengas).

The costs of publication of this article were defrayed in part by the payment of page charges. This article must therefore be hereby marked *advertisement* in accordance with 18 U.S.C. Section 1734 solely to indicate this fact.

We thank Rebecca Mosher, Sarah Waywell (Millennium Pharmaceuticals), Mila M. McCurrach, and Sagarika Ray (Cold Spring Harbor Laboratory) for help and advice with mouse xenografts at an early phase of this work; the following investigators at the University of Michigan: Laure Rittie for the analysis of gene expression by quantitative RT-PCR, James T. Elder and Rajan Nair for sequencing of *B-Raf* and *N-Ras*, and Audrey Bengston and Wen-Hua Tang for technical assistance; José Esteban, Gabriel Núñez, Mikhail Nikiforov, and Andrzej A. Dlugosz for helpful suggestions and critical reading of this article; Colin S. Duckett's laboratory for reagents and advice; and Brian Nickoloff (Loyola University) for sharing data before publication regarding the regulation of Noxa by bortezomib.

References

1. Grossman D, Altieri DC. Drug resistance in melanoma: mechanisms, apoptosis, and new potential therapeutic targets. Cancer Metastasis Rev 2001;20:3–11.
2. Houghton AN, Polsky D. Focus on melanoma. Cancer Cell 2002;2:275–8.
3. Ivanov VN, Bhoumik A, Ronai Z. Death receptors and melanoma resistance to apoptosis. Oncogene 2003;22:3152–61.
4. Soengas MS, Lowe SW. Apoptosis and melanoma chemoresistance. Oncogene 2003;22:3138–51.
5. Serrone L, Zeuli M, Sega FM, Cognetti F. Dacarbazine-based chemotherapy for metastatic melanoma: thirty-year experience overview. J Exp Clin Cancer Res 2000;19:21–34.
6. Lens MB, Eisen TG. Systemic chemotherapy in the treatment of malignant melanoma. Expert Opin Pharmacother 2003;4:2205–11.
7. Lawson DH. Update on the systemic treatment of malignant melanoma. Semin Oncol 2004;31:33–7.

8. Garber K. Cancer research. Taking garbage in, tossing cancer out? Science 2002;295:612–3.
9. Adams J. The development of proteasome inhibitors as anticancer drugs. Cancer Cell 2004;5:417–21.
10. Adams J. The proteasome: a suitable antineoplastic target. Nat Rev Cancer 2004;4:349–60.
11. Bross PF, Kane R, Farrell AT, et al. Approval summary for bortezomib for injection in the treatment of multiple myeloma. Clin Cancer Res 2004;10:3954–64.
12. Goy A, Gilles F. Update on the proteasome inhibitor bortezomib in hematologic malignancies. Clin Lymphoma 2004;4:230–7.
13. Lenz HJ. Clinical update: proteasome inhibitors in solid tumors. Cancer Treat Rev 2003;29:41–8.
14. Amiri KI, Horton LW, LaFleur BJ, Sosman JA, Richmond A. Augmenting chemosensitivity of malignant melanoma tumors via proteasome inhibition: implication for bortezomib (VELCADE, PS-341) as a therapeutic agent for malignant melanoma. Cancer Res 2004;64:4912–8.
15. Poetsch M, Dittberner T, Woenckhaus C. PTEN/MMAC1 in malignant melanoma and its importance for tumor progression. Cancer Genet Cytogenet 2001;125:21–6.
16. Yu J, Tiwari S, Steiner P, Zhang L. Differential apoptotic response to the proteasome inhibitor bortezomib [VELCADE, PS-341] in Bax-deficient and p21-deficient colon cancer cells. Cancer Biol Ther 2003;2:694–9.
17. Fahy BN, Schlieman MG, Virudachalam S, Bold RJ. Schedule-dependent molecular effects of the proteasome inhibitor bortezomib and gemcitabine in pancreatic cancer. J Surg Res 2003;113:88–95.
18. Mitsiades N, Mitsiades CS, Poulaki V, et al. Molecular sequelae of proteasome inhibition in human multiple myeloma cells. Proc Natl Acad Sci U S A 2002;99:14374–9.
19. Pham LV, Tamayo AT, Yoshimura LC, Lo P, Ford RJ. Inhibition of constitutive NF-κB activation in mantle cell lymphoma B cells leads to induction of cell cycle arrest and apoptosis. J Immunol 2003;171:88–95.
20. Frankel A, Man S, Elliott P, Adams J, Kerbel RS. Lack of multicellular drug resistance observed in human ovarian and prostate carcinoma treated with the proteasome inhibitor PS-341. Clin Cancer Res 2000;6:3719–28.
21. Satherley K, de Souza L, Neale MH, et al. Relationship between expression of topoisomerase II isoforms and chemosensitivity in choroidal melanoma. J Pathol 2000;192:174–81.
22. Sayers TJ, Brooks AD, Koh CY, et al. The proteasome inhibitor PS-341 sensitizes neoplastic cells to TRAIL-mediated apoptosis by reducing levels of c-FLIP. Blood 2003;102:303–10.
23. Satyamoorthy K, Meier F, Hsu MY, Berking C, Herlyn M. Human xenografts, human skin and skin reconstructs for studies in melanoma development and progression. Cancer Metastasis Rev 1999;18:401–5.
24. Soengas MS, Capodieci P, Polsky D, et al. Inactivation of the apoptosis effector Apaf-1 in malignant melanoma. Nature 2001;409:207–11.
25. McCurrach ME, Lowe SW. Methods for studying pro- and antiapoptotic genes in nonimmortal cells. Methods Cell Biol 2001;66:197–227.
26. Wilkinson JC, Cepero E, Boise LH, Duckett CS. Upstream regulatory role for XIAP in receptor-mediated apoptosis. Mol Cell Biol 2004;24:7003–14.
27. Lois C, Hong EJ, Pease S, Brown EJ, Baltimore D. Germline transmission and tissue-specific expression of transgenes delivered by lentiviral vectors. Science 2002;295:868–72.
28. Satyamoorthy K, DeJesus E, Linnenbach AJ, et al. Melanoma cell lines from different stages of progression and their biological and molecular analyses. Melanoma Res 1997;7:S35–42.
29. Ahmann DL, Bisel HF, Edmonson JH, et al. Clinical comparison of Adriamycin and a combination of methyl-CCNU and imidazole carboxamide in disseminated malignant melanoma. Clin Pharmacol Ther 1976;19:821–4.
30. Ridolfi R, Chiarion-Sileni V, Guida M, et al. Cisplatin, dacarbazine with or without subcutaneous interleukin-2, and interferon α-2b in advanced melanoma outpatients: results from an Italian multicenter phase III randomized clinical trial. J Clin Oncol 2002;20:1600–7.
31. Chapman PB, Einhorn LH, Meyers ML, et al. Phase III multicenter randomized trial of the Dartmouth regimen versus dacarbazine in patients with metastatic melanoma. J Clin Oncol 1999;17:2745–51.
32. Green DR, Kroemer G. The pathophysiology of mitochondrial cell death. Science 2004;305:626–9.
33. Nijhawan D, Fang M, Traer E, et al. Elimination of Mcl-1 is required for the initiation of apoptosis following ultraviolet irradiation. Genes Dev 2003;17:1475–86.
34. Chen L, Willis SN, Wei A, et al. Differential targeting of prosurvival Bcl-2 proteins by their BH3-only ligands allows complementary apoptotic function. Mol Cell 2005;17:393–403.
35. Pavey S, Johansson P, Packer L, et al. Microarray expression profiling in melanoma reveals a BRAF mutation signature. Oncogene 2004;23:4060–7.
36. Oda E, Ohki R, Murasawa H, et al. Noxa, a BH3-only member of the Bcl-2 family and candidate mediator of p53-induced apoptosis. Science 2000;288:1053–8.
37. Villunger A, Michalak EM, Coultas L, et al. p53- and drug-induced apoptotic responses mediated by BH3-only proteins puma and noxa. Science 2003;302:1036–8.
38. Seo YW, Shin JN, Ko KH, et al. The molecular mechanism of Noxa-induced mitochondrial dysfunction in p53-mediated cell death. J Biol Chem 2003;278:48292–9.
39. Qin JZ, Stennett L, Bacon P, et al. p53-independent NOXA induction overcomes apoptotic resistance of malignant melanomas. Mol Cancer Ther 2004;3:895–902.
40. Zheng B, Georgakis GV, Li Y, et al. Induction of cell cycle arrest and apoptosis by the proteasome inhibitor PS-341 in Hodgkin disease cell lines is independent of inhibitor of nuclear factor-κB mutations or activation of the CD30, CD40, and RANK receptors. Clin Cancer Res 2004;10:3207–15.
41. Bold RJ, Virudachalam S, McConkey DJ. Chemosensitization of pancreatic cancer by inhibition of the 26S proteasome. J Surg Res 2001;100:11–7.
42. Dong QG, Sclabas GM, Fujioka S, et al. The function of multiple IκB:NF-κB complexes in the resistance of cancer cells to Taxol-induced apoptosis. Oncogene 2002;21:6510–9.
43. Dai DL, Martinka M, Bush JA, Li G. Reduced Apaf-1 expression in human cutaneous melanomas. Br J Cancer 2004;91:1089–95.
44. Svingen PA, Loegering D, Rodriquez J, et al. Components of the cell death machine and drug sensitivity of the National Cancer Institute Cell Line Panel. Clin Cancer Res 2004;10:6807–20.
45. Zanon M, Piris A, Bersani I, et al. Apoptosis protease activator protein-1 expression is dispensable for response of human melanoma cells to distinct proapoptotic agents. Cancer Res 2004;64:7386–94.
46. Lowe SW, Cepero E, Evan G. Intrinsic tumour suppression. Nature 2004;432:307–15.
47. Olivier M, Eeles R, Hollstein M, Khan MA, Harris CC, Hainaut P. The IARC TP53 database: new online mutation analysis and recommendations to users. Hum Mutat 2002;19:607–14.

Differential Regulation of Noxa in Normal Melanocytes and Melanoma Cells by Proteasome Inhibition: Therapeutic Implications

Yolanda Fernández, Monique Verhaegen, Thomas P. Miller, et al.

Cancer Res 2005;65:6294-6304.